

## Functional and structural bases of a cysteine-less mutant as a long-lasting substitute for galectin-1

Nozomu Nishi<sup>1,2</sup>, Akemi Abe<sup>3</sup>, Jun Iwaki<sup>4</sup>,  
Hiromi Yoshida<sup>3</sup>, Aiko Itoh<sup>5</sup>, Hiroki Shoji<sup>2</sup>,  
Shigehiro Kamitori<sup>3</sup>, Jun Hirabayashi<sup>4</sup>, and  
Takanori Nakamura<sup>2</sup>

<sup>2</sup>Department of Endocrinology, Faculty of Medicine; <sup>3</sup>Division of Structural Biology, Life Science Research Center, Kagawa University, Kagawa 761-0793; <sup>4</sup>Research Center for Medical Glycoscience, National Institute of Advanced Industrial Science and Technology (AIST), Tsukuba Central 2, 1-1-1, Umezono, Tsukuba, Ibaraki 305-8568; and <sup>5</sup>GalPharma Co., Ltd., 2217-44 Hayashimachi, Takamatsu, Kagawa 761-0301, Japan

Received on April 24, 2008; revised on September 12, 2008; accepted on September 12, 2008

**Galectin-1 (Gal-1), a member of the  $\beta$ -galactoside-binding animal lectin family, has a wide range of biological activities, which makes it an attractive target for medical applications. Unlike other galectins, Gal-1 is susceptible to oxidation at cysteine residues, which is troublesome for in vitro/vivo studies. To overcome this problem, we prepared a cysteine-less mutant of Gal-1 (CSGal-1) by substituting all cysteine residues with serine residues. In the case of wild-type Gal-1, the formation of covalent dimers/oligomers was evident after 10 days of storage in the absence of a reducing agent with a concomitant decrease in hemagglutination activity, while CSGal-1 did not form multimers and retained full hemagglutination activity after 400 days of storage. Frontal affinity chromatography showed that the sugar-binding specificity and affinity of Gal-1 for model glycans were barely affected by the mutagenesis. Gal-1 is known to induce cell signaling leading to an increase in the intracytoplasmic calcium concentration and to cell death. CSGal-1 is also capable of inducing calcium flux and growth inhibition in Jurkat cells, which are comparable to or more potent than those induced by Gal-1. The X-ray structure of the CSGal-1/lactose complex has been determined. The structure of CSGal-1 is almost identical to that of wild-type human Gal-1, showing that the amino acid substitutions do not affect the overall structure or carbohydrate-binding site structure of the protein. These results indicate that CSGal-1 can serve as a stable substitute for Gal-1.**

**Keywords:** galectin/site-directed mutagenesis/thiol oxidation/X-ray crystallography

### Introduction

Galectins comprise a phylogenetically conserved family of animal lectins defined by an affinity for  $\beta$ -galactosides and

conserved sequence elements in the carbohydrate-binding site (Barondes et al. 1994). The family was originally designated as the S-type lectin family based on the requirement of a thiol (-SH) reducing agent for maintenance of the lectin activity of galectin-1 (Gal-1), the prototypic member of the galectin family. However, this property (high sensitivity to oxidation of -SH groups) is not shared by other members, being confined to Gal-1 so far. Gal-1 is ubiquitously but differentially expressed in normal and pathological animal tissues, and a variety of biological activities, including modulation of innate and adaptive immune responses, malignant progression of tumor cells, etc., has been reported for Gal-1 (Rabinovich et al. 2002, 2005; Camby et al. 2006). The biological activities of Gal-1, especially the modulation of immune responses, led to a novel approach for the treatment of immune-related diseases including hepatitis (Santucci et al. 2000), colitis (Santucci et al. 2003), arthritis (Rabinovich et al. 1999), and graft versus host disease (Baum et al. 2003), in which recombinant Gal-1 is used as a therapeutic agent.

In addition to its diverse biological roles as a lectin, oxidized Gal-1 with three intramolecular disulfide bonds, which lacks lectin activity, has been shown to promote axonal regeneration in peripheral nerves after axotomy (Horie et al. 1999; Inagaki et al. 2000). Oxidized Gal-1 is supposed to exert its action through stimulation of macrophages to secrete a factor that promotes axonal growth and Schwann cell migration (Horie et al. 2004). The authors also showed that an artificial mutant of Gal-1 (CSGal-1) in which all six cysteine residues were replaced by serine residues was resistant to oxidation in the absence of a reducing agent and inactive in promoting axonal regeneration (Inagaki et al. 2000). This cysteine-less Gal-1 molecule is a promising candidate for an oxidation-resistant stable substitute for Gal-1 for both in vitro and in vivo applications provided that the mutation does not change the sugar-binding specificity, and thus does not affect the biological activity as a lectin. Detailed characterization of CSGal-1, however, has not been reported until now. The aim of this study was to establish CSGal-1 as a long-standing agent essentially equivalent to wild-type Gal-1, except for oxidation-dependent acquisition of neurotrophic activity, by means of biochemical, cell biological and crystallographic analyses.

### Results

#### *Stability of the wild-type and mutant forms of Gal-1*

The wild-type Gal-1 and CSGal-1 were subjected to long-term stability testing. Another mutant form of Gal-1, Gal-1Cys3Ser (Gal-1C3S), was also tested and compared with Gal-1 and CSGal-1 because the C3S mutation had been reported to greatly increase the stability of Gal-1 (Hirabayashi and Kasai 1991). All the recombinant proteins were successfully expressed

<sup>1</sup>To whom correspondence should be addressed: Tel: +81-87-891-2107; Fax: +81-87-891-2108; e-mail: nnishi@med.kagawa-u.ac.jp

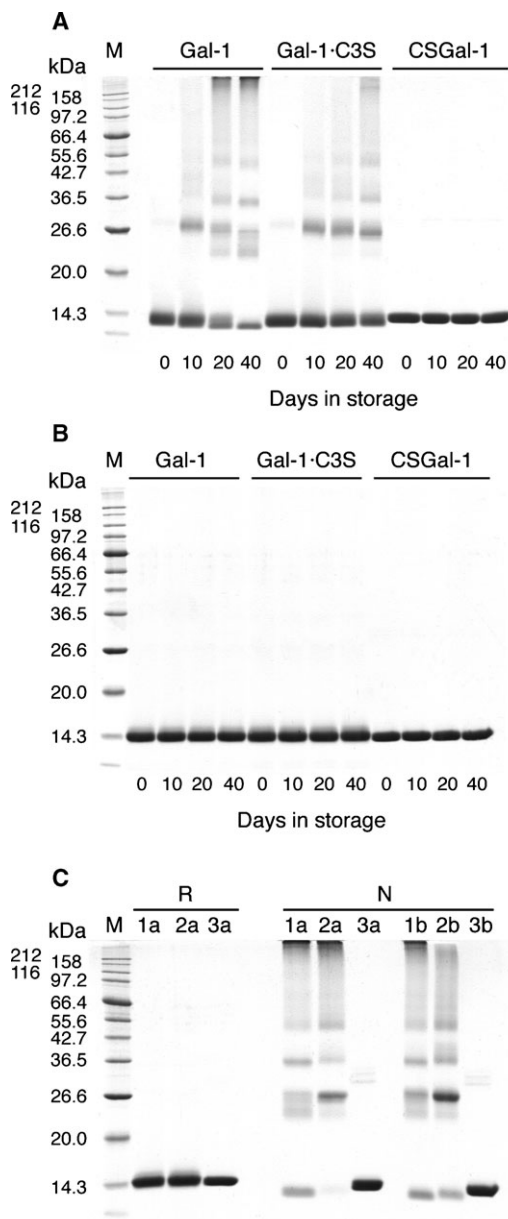


**Fig. 1.** Long-term stability of the wild-type and mutant forms of Gal-1. (A and B) Purified recombinant proteins dissolved in PBS were stored at 4°C under sterile conditions. Samples were withdrawn at the indicated time points and then subjected to SDS-PAGE under nonreducing (A) and reducing conditions (B). (C) Purified recombinant proteins dissolved in PBS (a) and PBS, 1 mM DTT (b) were stored for 400 days at 4°C under sterile conditions. Samples were analyzed by SDS-PAGE under reducing (R) and nonreducing (N) conditions. Lanes 1a and 1b, Gal-1; lanes 2a and 2b, Gal-1-C3S; lanes 3a and 3b, CSGal-1. M, molecular weight marker proteins.

as tag-free forms in *Escherichia coli* (*E. coli*) and purified by lactose-affinity chromatography to apparent homogeneity (Figure 1A and B). A typical yield of about 40 mg purified protein from one liter of culture was obtained for all the proteins. Long-term stability was assessed over a 400-day period at 4°C under sterile conditions. Sodium dodecyl sulfate – polyacrylamide gel electrophoresis (SDS-PAGE) analysis under nonreducing conditions showed that the formation of a covalent

**Table I.** Effect of long-term storage on hemagglutination activity of the wild-type and mutant forms of galectin-1

Storage time (days)	Minimum concentration for hemagglutination (nM)					
	Gal-1		Gal-1-C3S		CSGal-1	
	+ <sup>a</sup>	- <sup>b</sup>	+	-	+	-
0	100	100	100	100	100	100
4	100	200	100	100	100	100
10	100	400	100	100	100	100
20	400	800	200	200	100	100
40	400	1600	200	400	100	100
400	>6400	>6400	>6400	>6400	100	100

The purified recombinant proteins were dissolved in PBS, 1 mM DTT or PBS, and stored at 4°C under sterile conditions.

<sup>a</sup>Stored in PBS, 1 mM DTT.

<sup>b</sup>Stored in PBS.

valent dimer (28-kDa band) was evident for Gal-1 and Gal-1C3S after 10 days of storage in the absence of a reducing agent (Figure 1A and B). The contents of higher molecular weight forms (covalent oligomers) increased with the storage time. The addition of 1 mM dithiothreitol (DTT) to the storage buffer greatly reduced the oxidation of Gal-1 and Gal-1C3S upon storage for at least 20 days, but oxidation products gradually increased thereafter (data not shown). On the other hand, the oxidation product of CSGal-1 was not detectable after 400 days of storage in the absence of a reducing agent (Figure 1C). The changes in the hemagglutination titers of the recombinant proteins during storage were consistent with the formation of the oxidation products (Table I).

#### Sugar-binding specificity of CSGal-1

We previously examined the sugar-binding specificity of Gal-1 in comparison with those of other galectins by frontal affinity chromatography (FAC) analysis using 41 pyridylaminated-oligosaccharides (PA-oligosaccharides) (Hirabayashi et al. 2002). In the present study, we carried out more extensive analyses of the sugar-binding specificities of Gal-1 and CSGal-1 using 120 PA-oligosaccharides to determine whether the Cys-to-Ser mutations have any effect on the specificity of Gal-1. The results shown in Figure 2 indicate that there is no noticeable difference between Gal-1 and CSGal-1 regarding the sugar-binding specificity or affinity for all the PA-oligosaccharides, and the following features are evident in terms of the sugar-binding characteristics of Gal-1 (and CSGal-1). (i) Gal-1 showed extensive affinity for complex-type *N*-glycans. The affinity increased with an increase in the branching number up to triantennary *N*-glycans, whereas the affinity for functionally monovalent *N*-glycans was low. (ii)  $\alpha$ 2-6 Sialylation completely abolished the affinity. (iii) Other than basic saccharides, Gal-1 showed affinity for Galili pentasaccharide, lacto-*N*-fucopentaose I (LNFP-I) and A-hexasaccharide. (iv) Gal-1 did not show any particular preference for repeated *N*-acetylglucosamine structures. These results are consistent with our previous report (Hirabayashi et al. 2002).

#### Biological activity of CSGal-1

Gal-1 is known to act as a mitogen, as an inhibitor of cell proliferation, and as a promoter of apoptosis depending on the cell type and assay conditions (Scott and Weinberg 2004). The

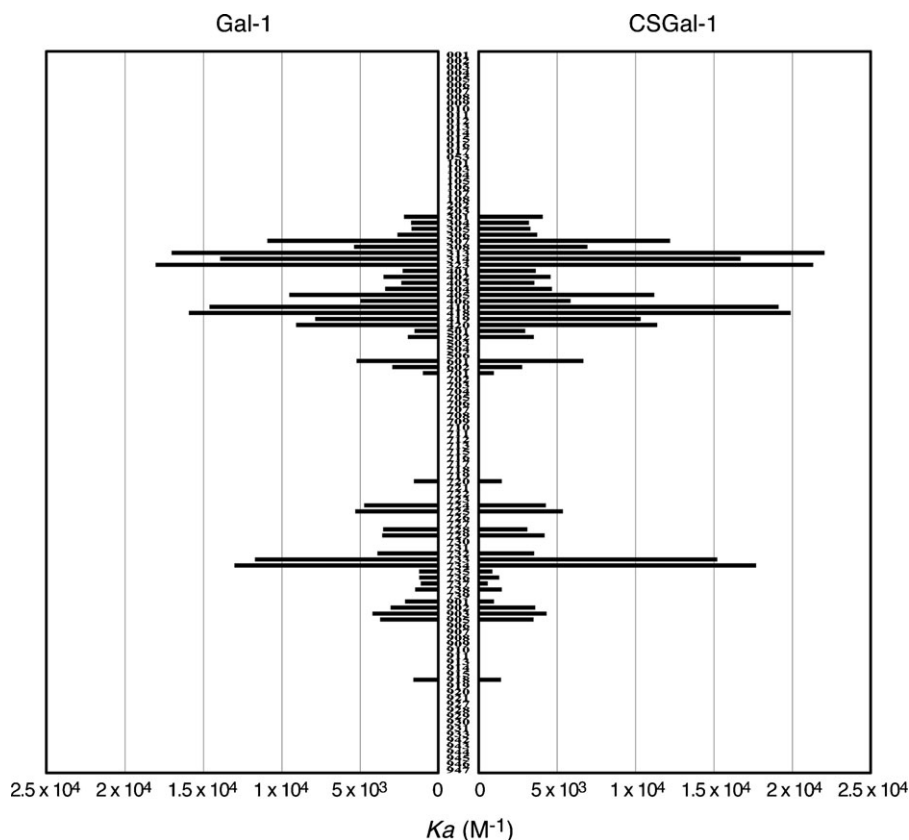


**Fig. 2.** FAC analysis of the carbohydrate-binding specificities of Gal-1 (left panel) and CSGal-1 (right panel). Results are expressed as affinity constants ( $K_a$ ). The numbers between the two graphs represent sugar numbers indicated in Supplementary Figure 1.

ability of Gal-1 to induce apoptosis in activated T lymphocytes is the most notable among the cell survival and proliferation-related activities of Gal-1 (Perillo et al. 1995). In Jurkat T-cells, Gal-1 triggers a sustained increase in the intracytoplasmic calcium concentration and induces apoptosis (Walzel et al. 2000, 2006). CSGal-1 stimulated intracytoplasmic calcium flux in a similar manner to Gal-1 (Figure 3A and B). The ability of CSGal-1 to induce calcium flux was retained after 400 days of storage in the absence of a reducing agent whereas Gal-1 was completely inactivated (Figure 3C). Although induction of calcium flux is not always associated with apoptotic/nonapoptotic cell death (Pace et al. 2000; Lu et al. 2007), treatment with Gal-1 resulted in overall growth inhibition in Jurkat cells in the presence, but not in the absence, of DTT in the culture medium (Figure 4A and B). On the other hand, CSGal-1 induced growth inhibition of the cells irrespective of the presence of DTT, and the effect was more potent than that of Gal-1.

#### *Binding specificity of CSGal-1 for membrane glycoproteins*

A variety of binding partners for Gal-1, including cell membrane proteins and extracellular matrix proteins, have been reported in conjunction with its multiple biological roles (Elola et al. 2005). In the case of apoptosis/cell death-related activity, CD2, CD3, CD7, CD43, and CD45 have been identified as functional receptors (Pace et al. 2000; Walzel et al. 2000; Nguyen et al. 2001; Hernandez et al. 2006). To compare the binding specificities of Gal-1 and CSGal-1 for membrane glycoproteins, solubilized Jurkat cell membrane proteins were subjected to affinity purifi-

cation on a Gal-1/CSGal-1-immobilized column. The proteins eluted from the column with lactose but not with sucrose were analyzed by SDS-PAGE. The electrophoretic patterns of the eluates were closely similar to each other, high-molecular-weight bands corresponding to about 200 kDa being abundant (Figure 5A). Western blot analysis showed that all the candidate receptor proteins (CD2, CD3, CD7, CD43, and CD45) were detectable and present in similar amounts in the eluates from the Gal-1- and CSGal-1-immobilized columns (Figure 5B).

#### *X-ray structure of the CSGal-1/lactose complex*

There are two molecules (Mol-A and Mol-B) of CSGal-1 in an asymmetric unit, a homo-dimer being formed. In Ramachandran plots (Ramachandran and Sasisekharan 1968), 90.4% of all residues in Mol-A and 86.9% of those in Mol-B were shown to be in the most favored regions, and there were no residues in the generously allowed and disallowed regions, as determined with the program PROCHECK (Laskowski et al. 1992). The final ( $2F_o - F_c$ ) electron density map showed that almost all the atoms of the protein molecules, each of which comprises 134 amino acid residues, a bound lactose molecule and solvent molecules, were nicely fitted, except for the N-terminus residue (Ala2). All substitutions of Cys with Ser were confirmed by inspection of the electron density map. The average B-factors were 18.8 Å<sup>2</sup> (protein), 26.2 Å<sup>2</sup> (lactose), 24.8 Å<sup>2</sup> (solvent), and 24.0 Å<sup>2</sup> (O $\gamma$  of Ser replacing Cys).

The monomer of CSGal-1 adopts a  $\beta$ -sandwich structure formed by two antiparallel  $\beta$ -sheets consisting of six (S1-S6)

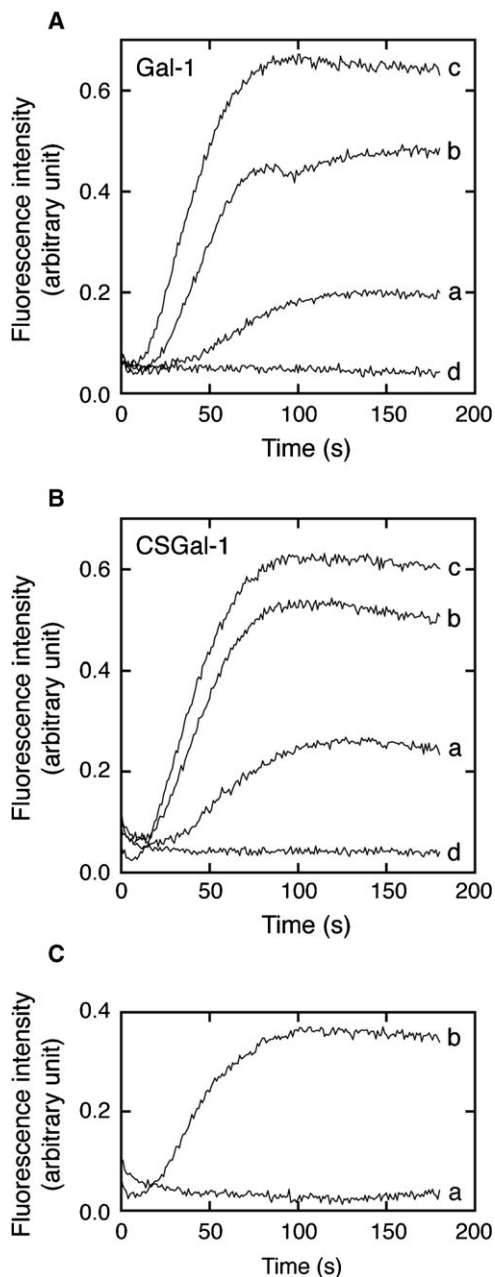


**Fig. 3.** Intracellular calcium mobilization induced by Gal-1 and CSGal-1 in Jurkat cells. Jurkat cells were loaded with fluo-3-AM for 1 h at 37°C. After washing with a recording medium, cytosolic calcium was monitored as the fluorescence of fluo-3 using a fluorescence spectrophotometer. (A and B) Increases in intracellular calcium concentration induced by Gal-1 (A) and CSGal-1 (B). The cells were treated with 1  $\mu$ M Gal-1/CSGal-1 (a), 3  $\mu$ M Gal-1/CSGal-1 (b), and 10  $\mu$ M Gal-1/CSGal-1 (c, d) in the absence (a–c) and presence (d) of 20 mM lactose. (C) Increases in the intracellular calcium concentration induced by 3  $\mu$ M Gal-1 (a) and CSGal-1 (b) stored for 400 days at 4°C in the absence of DTT.

and five (F1–F5)  $\beta$ -strands, respectively, and on dimerization, pairs of the same  $\beta$ -sheets are connected to give two large antiparallel  $\beta$ -sheets, as shown in Figure 6A. The nomenclature for  $\beta$ -strands follows that for wild-type human Gal-1, the  $\beta$ -strands being aligned in the sequence of S1, F2, S3, S4, S5, S6a/S6b, F3, F4, F5, S2 and F1 from the N- to the C-terminus (Lopez-

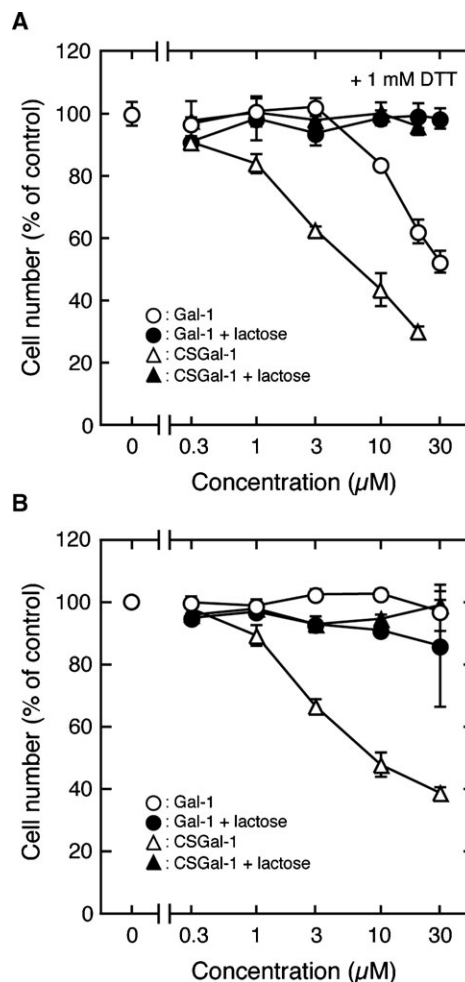


**Fig. 4.** Comparison of the antiproliferative activities of Gal-1 and CSGal-1. The antiproliferative effect on Jurkat cells was determined by means of the WST-8 assay. (A) Jurkat cells were cultured in the presence of an assay sample and 1 mM DTT with or without 20 mM lactose for 24 h. After the addition of WST-8 reagent, the culture was continued for 2 h. The viable cell number was determined with an automated plate reader. DTT (1 mM) itself showed no effect on growth of Jurkat cells under the conditions used. (B) The experimental conditions were the same as in A except that DTT was not added to the culture medium. The viable cell number of an untreated control culture was taken as 100%. The results represent the means  $\pm$  SD of triplicate measurements.

Lucendo et al. 2004). The carbohydrate-binding sites are located at the ends of a dimer. However, for the CSGal-1/lactose complex structure, the electron density of the bound lactose molecule of Mol-A can be clearly identified at the carbohydrate-binding site, while there is no corresponding electron density for Mol-B. This may be due to a crystal packing effect, as discussed later. A lactose molecule binds to the concave surface formed by S4, S5, and S6 in Mol-A, as shown in Figure 6B. The galactose moiety is fixed between His53 and Trp69 through stacking interactions and is strictly recognized as seven hydrogen bonds with amino acid residues: O-2–His53, O-4–His45, O-4–Asn47, O-4–Arg49, O-5–Arg49, O-6–Asn62 and O-6–Glu72. On the other hand, in the glucose moiety, only the O-3 atom makes two hydrogen bonds with Arg49 and Glu72, and the reducing end

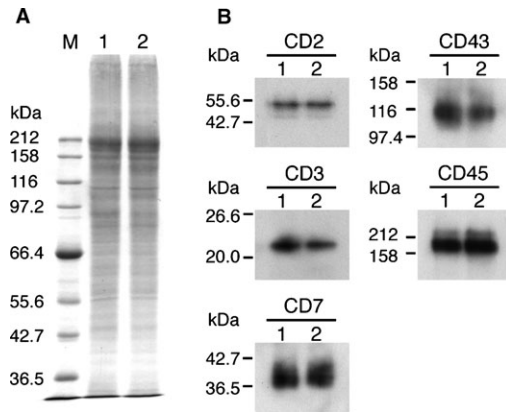


**Fig. 5.** Comparison of Gal-1 and CSGal-1 binding proteins in Jurkat cells. Gal-1 and CSGal-1 binding proteins were affinity-purified from the solubilized membrane fraction of Jurkat cells using a Gal-1/CSGal-1-immobilized column. (A) The affinity-purified proteins were resolved by means of SDS-PAGE and then stained with Coomassie Brilliant Blue R-250. (B) The affinity-purified proteins were subjected to Western blot analysis using antibodies against the candidate receptor proteins for Gal-1. Lane 1, the affinity-purified proteins with the Gal-1-immobilized column; lane 2, the affinity-purified proteins with the CSGal-1-immobilized column. M, molecular weight marker proteins.

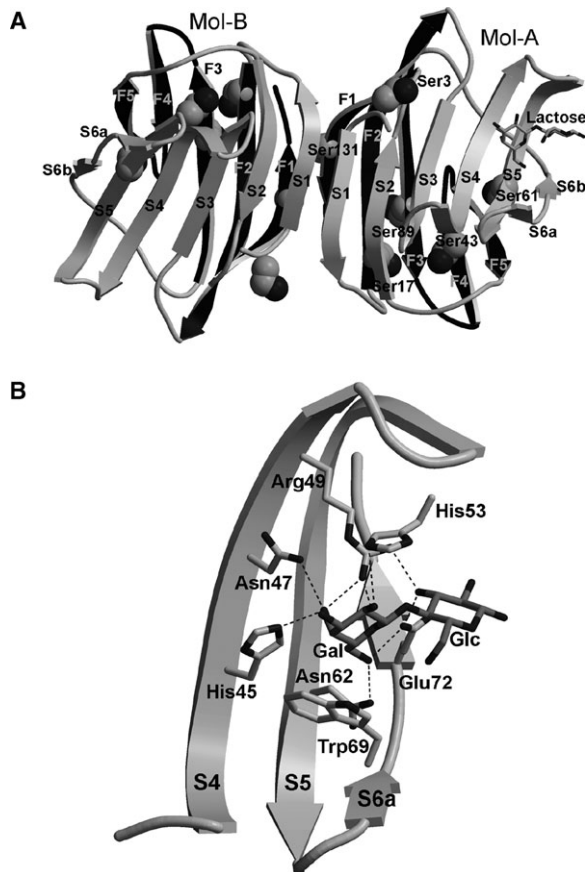


**Fig. 6.** X-ray crystallographic structure of CSGal-1. (A) The overall structure of CSGal-1 revealed with the programs MOLSCRIPT (Kraulis 1991) and Raster3D (Merritt and Bacon 1997). The front  $\beta$ -sheet (S1 – S6a/S6b) and back  $\beta$ -sheet (F1–F5) are shown in white and dark gray, respectively. The bound lactose molecule and Ser residues replacing Cys residues are shown as stick and space-filling models, with the oxygen atoms in dark gray. (B) The structure of the carbohydrate-binding site of Mol-A revealed with the programs MOLSCRIPT and Raster3D. The oxygen and nitrogen atoms are shown in dark gray, and the hydrogen bonds are indicated by dashed lines.

side of the glucose moiety is extensively exposed on the solvent accessible surface.

There are six Ser residues replacing Cys residues, as shown in Figure 6A. Ser3 in the N-terminal loop, Ser17 in F2, Ser89 in F3, and Ser 131 in F1 direct their side-chain groups toward the outside of the protein, forming many hydrogen bonds with solvent molecules, and Ser43 in S4 and Ser61 in S5 direct their side-chain groups toward the inside of the protein, being surrounded by hydrophobic residues, like the Cys residues in wild-type human Gal-1. Almost all the Ser residues adopt the same side-chain conformation as the Cys residues, except Ser16 in Mol-A and Ser43 in both molecules, where hydrogen bonds are newly found: Ser17 (O $\gamma$ ), Thr90 (O $\gamma$ ) in Mol-A and Ser43 (O $\gamma$ ), solvent molecule in both molecules.

## Discussion

All Gal-1 characterized in mammals contains six conserved cysteine residues. Spontaneous intramolecular disulfide bonding of the cysteine residues occurs predominantly between Cys3 and Cys131, Cys17 and Cys89, and Cys43 and Cys61 under oxidative conditions (Tracey et al. 1992). In addition to intramolecular disulfide bonding, an intermolecular reaction resulting in dimer/oligomer formation has also been reported (Hirabayashi and Kasai 1991). In the present study, we performed SDS-PAGE under nonreducing conditions to assess the formation of oxidation products of the wild-type and mutant Gal-1 proteins. Although the detection of Gal-1 species with only intramolecular disulfide bond(s) is difficult with this method, the increase in the high-molecular-weight species, i.e., Gal-1 molecules with intermolecular disulfide bond(s), coincided with the decreases in the hemagglutination titers of the recombinant proteins during storage. It is not likely, therefore, that intramolecular disulfide bond formation is substantially favored over intermolecular reaction under the storage conditions used. The oxidation of Gal-1 and Gal-1C3S was delayed for at least 20 days by the addition of 1 mM DTT (data not shown). The addition of higher concentrations or periodic addition of DTT to the storage medium may protect Gal-1 against oxidation for a longer period. However, high concentrations of DTT are not compatible with some applications and it is not feasible to maintain the DTT (reduced form) concentration at an effective level.

Lopez-Lucendo et al. (2004) reported that the C2S mutation (designated as the C3S mutation in the present paper) affects the sugar-binding property of Gal-1. In their crystallographic study on the wild-type and mutant Gal-1, two single mutations (C2S and R111H) introduced at some distance from the carbohydrate recognition motif were found to influence the interactions with lactose and *N*-acetyllactosamine. They argued that this effect revealed the occurrence of long-range alterations in the Gal-1 conformation. It is possible that all the Cys-to-Ser mutations including the C3S mutation have minor effects on the folding of Gal-1. It has been established, based on site-directed mutagenesis and X-ray crystallographic studies, that the eight most conserved amino acid residues in the galectin family (His45, Asn47, Arg49, Val60, Asn62, Trp69, Glu72, and Arg74 of human Gal-1) undergo direct interaction with the sugar molecule, i.e., they form sugar-binding sites. Two out of the six cysteine residues of Gal-1 (Cys43 and Cys61) are located in close proximity to the sugar-binding sites, and thus substitution of

these cysteine residues may affect the interaction between Gal-1 and sugar chains. Analysis of the sugar-binding properties of Gal-1 and CSGal-1 by FAC in the present study, however, clearly showed that CSGal-1 has essentially the same sugar-binding specificity and affinity as Gal-1. These results suggest that the effect, if any, of the Cys-to-Ser mutations does not substantially alter the oligosaccharide-Gal-1 interactions in solution.

The observation that Gal-1 could induce apoptosis in activated T lymphocytes has established Gal-1 as a novel proapoptotic factor, although the activity was demonstrated with relatively high concentrations (Perillo et al. 1995). In addition to activated T lymphocytes, several T-cell lines including Jurkat T-cells are susceptible to Gal-1-induced apoptosis/cell death. In Jurkat cells, Gal-1 augments rapid intracellular calcium mobilization, which is sensitive to lactose and *N*-glycan processing inhibitors, through transient release from intracellular stores and an altered influx across the plasma membrane (Walzel et al. 2000). Although it is not clear whether calcium flux is a prerequisite for Gal-1-induced cell death in Jurkat cells, calcium-mobilizing activity can serve as an indication of the biological activity of Gal-1 in whole cells. Recently, Cummings and his colleagues demonstrated that Gal-1 induces apoptosis in MOLT-4 cells only in the presence of DTT (Stowell et al. 2007). They suggested that Gal-1-induced apoptosis in the presence of DTT results from alterations in cellular physiology and not a requirement to preserve Gal-1 activity under oxidative conditions, although the precise mechanism is unclear. We compared the effects of Gal-1 and CSGal-1 on the growth of Jurkat cells both in the presence and absence of DTT in addition to their calcium-mobilizing activities to assess the influence of the Cys-to-Ser mutations. CSGal-1 induced calcium flux to a level comparable to that induced by Gal-1, and the activity remained almost unchanged after 400 days of storage, which is consistent with the results of the stability test. Gal-1 and CSGal-1 suppressed the growth of Jurkat cells in the presence of DTT and the effect of CSGal-1 was significantly higher than that of Gal-1. It is possible that partial oxidation of Gal-1 occurs during 24 h incubation in the culture medium, even in the presence of DTT. The oxidative inactivation of Gal-1 may partly explain the difference. The growth-inhibiting effect of Gal-1 was not observed in the absence of DTT in accordance with the results of Stowell et al. However, in the case of CSGal-1, the growth-inhibiting activity was hardly affected by omission of DTT. The role of DTT in Gal-1-induced apoptosis (i.e., alterations in cellular physiology) was hypothesized based on the observations that C2S-Gal-1 (designated as Gal-1C3S in the present paper) induced apoptosis of MOLT-4 cells in the presence, but not in the absence, of DTT and that glutathione, a cell-impermeable reducing agent, could not substitute for DTT in supporting the apoptosis-inducing activity of Gal-1 (Stowell et al. 2007). Although C2S-Gal-1/Gal-1C3S was used as an oxidation-resistant mutant of Gal-1 in their study, Gal-1C3S is not stable under oxidative conditions, as shown in Figure 1 and Table I. In addition, it is not clear whether glutathione can protect Gal-1 against oxidation as effectively as DTT in the cell culture medium. The present finding, i.e., CSGal-1 suppressed the growth of Jurkat cells in the absence of DTT, suggests that Gal-1 exhibits intrinsic growth-inhibiting activity toward at least some cell types. Nevertheless, we do not exclude the possibility that the Cys-to-Ser mutations modify the biological activity of Gal-1, and therefore the results obtained

using CSGal-1 as a substitute for wild-type Gal-1 should be carefully interpreted.

FAC analysis revealed that the Cys-to-Ser mutations hardly affected the sugar-binding properties of Gal-1. As the analysis was carried out using model oligosaccharides, it cannot be ruled out that the mutations affect the interaction of Gal-1 with oligosaccharide chains attached to glycoproteins including Gal-1 receptors. Affinity isolation of Gal-1/CSGal-1 interacting proteins from solubilized Jurkat cell membrane showed that Gal-1 and CSGal-1 could interact with membrane glycoproteins in closely similar manners. Although quantitative data cannot be obtained by the method used (affinity purification), the biological activities of Gal-1 and CSGal-1 suggest that CSGal-1 can properly interact with the oligosaccharide moieties of Gal-1 receptor glycoproteins.

The rms deviation for C $\alpha$  atoms is 0.41 Å between CSGal-1 and wild-type human Gal-1 (PDB code 1GZW), and the interactions between the proteins and the bound lactose molecule in Mol-A are equivalent to each other. The displacement of C $\alpha$  atoms of the Ser residues replacing Cys residues are in the range of 0.130–0.791 Å, the mean being 0.396 Å, and the maximum C $\alpha$  atom displacement of 2.25 Å was found for Glu116 of Mol-B, it being 27 Å from the carbohydrate-binding site. Therefore, the substitution of the six Cys residues with Ser residues did not affect the overall structure or the carbohydrate-binding site structure of the protein, although a few hydrogen bonds with Ser17 and Ser43 are newly found in CSGal-1. In the crystal structure of CSGal-1, a lactose molecule is not found in Mol-B. The least-square fit of Mol-A with the lactose bound to Mol-B showed that the lactose molecule superimposed on Mol-B possibly interacts with the amino acid residues in the same manner as in the case of Mol-A. The rms deviation for C $\alpha$  atoms of carbohydrate-binding residues, His45, Asn47, Arg49, His53, Asn62, Trp69, and Glu72, is 0.37 Å, and the side-chain conformations of the residues are the same in Mol-A and Mol-B. However, in a crystal, the carbohydrate-binding site of Mol-B is partially occupied by the amino acid residues of the symmetry-operated molecule, and the superimposed lactose molecule makes slightly unusual contacts with Asn51 (3.2 Å, C-6 – O $\delta$ 1) and Ala56 (2.9 Å, O-6 – C $\beta$ ) of the symmetry operated Mol-A. It is expected that the bound lactose molecule in Mol-B is likely released from the protein in the process of crystallization. In the wild-type human Gal-1, the bound lactose molecules are found in both Mol-A and Mol-B (Lopez-Lucendo et al. 2004). This is because the two crystal structures are slightly different from each other:  $P2_12_12_1$ ,  $a = 36.93$ ,  $b = 87.43$ ,  $c = 95.70$  Å for CSGal-1 and  $P2_12_12_1$ ,  $a = 36.98$ ,  $b = 88.81$ ,  $c = 93.94$  Å for the wild-type human Gal-1, giving different intermolecular contacts between two crystals. In the crystal of the wild-type human Gal-1, the symmetry-operated Mol-A does not make any unusual contacts with the bound lactose molecule in Mol-B. The maximum displacement of the C $\alpha$  atom of Glu116 of Mol-B is also caused by the different intermolecular contacts. In CSGal-1, Glu116 of Mol-B forms van der Waals contacts with Pro78, Phe79, and Gln80 of symmetry-operated Mol-B, while in the wild-type human Gal-1, it undergoes the solvent-mediated interactions with the symmetry-operated Mol-B. This may be due not to the difference in the protein structure but to that in the crystallization conditions: pH = 7.0 for CSGal-1 and pH = 5.6 for the wild-type human Gal-1.

The present study was undertaken to establish CSGal-1, the potential advantage of which was first reported by Inagaki et al. (2000), as a long-standing substitute for wild-type Gal-1. The results obtained on biochemical, cell biological, and crystallographic analyses led to the conclusion that CSGal-1 can be an excellent substitute for Gal-1 as a lectin for both basic research and clinical applications. It may be interesting to conduct knock-in experiments with CSGal-1 to evaluate the biological significance of the oxidation-dependent acquisition of the neurotrophic activity of Gal-1.

## Material and methods

### Construction of expression vectors

In the present paper, the amino-terminal methionine residue corresponding to the start codon, which is known to be removed from the naturally occurring Gal-1 molecule, is assigned as residue 1. The following forward (F) and reverse (R) primers were used to amplify the cDNAs for the wild-type and site-directed mutants of galectin-1:

G1-F1, 5'-CGTCCTCATATGGCTTGTGGTCTGGTCCG C-3';

G1-R1, 5'-CGACCGGGATCCTCAGTCAAAGGCCACA CATT-3';

G1CS-F1, 5'-CGTCCTCATATGGCTAGCGGTCTGGT CGCCAGC-3';

G1CS-F1, 5'-CGTCCTCATATGGCTAGCGGTCTGGT GCCAGCAACCTGAATCTCAAACCTGGAGAGAGCC TT-3';

G1CS-R1, 5'-CGACCGCTCGAGTCAGTCAAAGGCCA CGCTTTT-3';

G1CS-F2, 5'-AACCTGAGCCTGCACTTCAACCCTCG CTTCAACGCCACGGCGACGCCAACACCATCGTG AGCAACAGC-3';

G1CS-R2, 5'-GCTGTTGCTCACGATGGTGTGGCGT CGCCGTGGCGTTGAAGCGAGGGTTGAAGTGCAG GCTCAGGT-3';

G1CS-F3, 5'-GCAGAGGTGAGCATCACCTTCGAC-3';

G1CS-R3, 5'-GTCGAAGGTGATGCTCACCTCTGC-3';

The cDNAs for human Gal-1 and a mutant Gal-1 carrying a single mutation (Cys3Ser) were amplified from first-strand cDNA prepared from the poly (A)<sup>+</sup>RNA fraction of the Jurkat T-lymphocytic cell line by polymerase chain reaction (PCR) using a forward primer tagged with an extra 5' *NdeI* sequence (G1-F1/G1CS-F1) and a reverse primer tagged with an extra *BamHI* sequence (G1-R1). The amplified cDNAs were digested with *NdeI* and *BamHI*, and then inserted into the *NdeI-BamHI* sites of pET-11a (Stratagene, La Jolla, CA). Site-directed mutagenesis of all cysteine residues (Cys3, 17, 43, 61, 89, and 131) of Gal-1 to serine residues was carried out as follows: in two separate reactions, two overlapping cDNA fragments corresponding to the N- and C-terminal halves of G1 were amplified using G1CS-F1 (with C3, 17S mutations) + G1CS-R2 (with C43, 61S mutations), and G1CS-F2 (with C43, 61S mutations) + G1CS-R1 (with a C131S mutation). The amplified fragments were then mixed and subjected to a second round of PCR using G1CS-F1 + G1CS-R1 to generate a full-length cDNA with five

point mutations (C3, 17, 43, 61, and 131S). The amplified cDNA was digested with *NdeI* and *BamHI*, and then inserted into the *NdeI-BamHI* sites of pET-11a. The last mutation (Cys89Ser) was introduced by means of essentially the same procedure using G1CS-R3 and G1CS-F3 as internal primers, and the plasmid prepared in the previous step as a target. The amplified cDNA carrying all the mutations was digested with *NdeI* and *BamHI*, and then inserted into the *NdeI-BamHI* sites of pET-11a. The DNA sequences of all the expression vectors were confirmed by automated sequencing.

### Expression and purification of recombinant proteins

Expression of tag-free recombinant proteins in *E. coli* BL21(DE3) cells was carried out as described previously (Lu et al. 2007). Recombinant proteins were purified by affinity chromatography on a lactose-agarose column (Seikagaku Co., Tokyo, Japan). The affinity-purified proteins were dialyzed against phosphate-buffered saline (PBS) and then sterilized by filtration unless otherwise specified. The protein concentrations were determined using BCA protein assay reagent (Pierce Biotechnology, Inc., Rockford, IL) and bovine serum albumin as a standard.

### Hemagglutination assays

Hemagglutination activity was assessed by the method of Nowak et al. (1976). Briefly, assay samples were prepared by serial twofold dilution of recombinant proteins in a 96-well microtiter plate. After the addition of bovine serum albumin and glutaraldehyde-fixed trypsin-treated rabbit erythrocytes to final concentrations of 0.25% (w/v) and 1% (v/v), respectively, the reaction mixture was incubated for 1 h at room temperature. The minimum concentration required for hemagglutination was visually determined.

### Frontal affinity chromatography

The interactions between Gal-1/CSGal-1 and PA-oligosaccharides were studied by FAC. The recombinant proteins dissolved in 0.1 M NaHCO<sub>3</sub> (pH8.3), 0.5 M NaCl were coupled to NHS-activated Sepharose 4 Fast Flow following the manufacturer's instructions. The galectin-immobilized Sepharose beads were packed into a stainless steel column (4 × 10 mm). Determination of the elution volume of the analyte and calculation of the *K<sub>d</sub>* value were carried out as described previously (Nakamura-Tsuruta et al. 2006).

### Cell culture and cell proliferation assay

The Jurkat T-cell line was obtained from the American Type Culture Collection (Manassas, VA). The cells were cultured in RPMI-1640 medium supplemented with 10% FBS, 100 mU/mL penicillin, and 100 µg/mL streptomycin at 37°C under a 5% CO<sub>2</sub>-95% air atmosphere. The antiproliferative effect on the Jurkat T-cell line was determined by means of the WST-8 assay. Jurkat cells (5 × 10<sup>4</sup> cells in 90 µL of medium/well) were plated on 96-well plates, and then cultured for 2 h. Test samples were added at various concentrations, and then the cultures were continued for 24 h. In some experiments, DTT was added to the culture medium with test samples at a final concentration of 1 mM. WST-8 reagent (Cell Counting Kit-8; Dojin Laboratories, Kumamoto, Japan) was added to the culture

medium (10  $\mu$ L/well), followed by incubation for 2 h. Each assay was performed in triplicate. Using an enzyme-linked immunoadsorbent assay autoreader, the viable cell number was determined by measuring the difference between the absorbance at 450 and that at 620 nm.

#### *Ca<sup>2+</sup> mobilization assay*

Calcium mobilization in Jurkat cells was determined by using Calcium Kit-Fluo3 (Dojin Laboratories). Jurkat cells were washed with PBS and then loaded with fluo-3-AM for 1 h at 37°C. After washing with a recording medium, the cells were suspended in a fresh recording medium. Cytosolic calcium was monitored as the fluorescence of fluo-3 using a fluorescence spectrophotometer.

#### *Affinity purification of Gal-1/CSGal-1-interacting proteins from solubilized Jurkat cell membrane*

Jurkat cells washed with PBS were suspended in 10 mM Tris-HCl (pH 7.5), 1 mM phenylmethylsulfonyl fluoride (PMSF) ( $4 \times 10^8$  cells/40 mL), followed by a single freeze-thaw cycle and sonication. The total membrane fraction was isolated by centrifugation at  $50,000 \times g$  for 30 min, and then washed sequentially with 20 mM Tris-HCl (pH 7.5), 0.15 M NaCl, 0.1 M lactose (TBS/lactose), and TBS to remove intrinsic galectins. The washed membrane fraction was homogenized with 20 mM Tris-HCl (pH 7.5), 0.5 M NaCl, 1% Triton X-100, 1 mM PMSF using a Teflon-glass homogenizer. After incubation for 1 h at 4°C with stirring, the homogenate was centrifuged as above. The resulting supernatant (solubilized membrane fraction) was subjected to affinity purification on a Gal-1/CSGal-1-immobilized column (about 4 mg of recombinant protein immobilized on 1 mL of HiTrap NHS-activated Sepharose). After washing the column with TBS, 0.2 M sucrose, Gal-1/CSGal-1-interacting proteins were eluted with TBS, 0.2 M lactose.

#### **Western blot analysis**

Samples were subjected to SDS-PAGE on 10% (for detection of CD43 and CD45) or 12.6% (CD2, CD3 and CD7) gels. The separated proteins were transferred to polyvinylidene difluoride membranes (Millipore Co., Billerica, MA), followed by immunodetection with monoclonal antibodies against human CD2 (MT210), CD3 (UCH-T1), CD7 (H-126), CD43 (DF-T1) (Santa Cruz Biotechnology, Santa Cruz, CA), and human CD45 (Chemicon International Inc., Temecula, CA), and phosphatase-labeled goat anti-mouse IgG antibodies (Kirkegaard and Perry Laboratories, Inc., Gaithersburg, MD), as described previously (Nishi et al. 1995).

#### *X-ray structure determination*

Crystallization of the CSGal-1/lactose complex was performed based on the conditions for human Gal-1 (Lopez-Lucendo et al. 2004). A suitable-sized crystal of the CSGal-1/lactose complex was grown by the vapor diffusion method in a drop comprising equal volumes of the protein solution (10 mg/mL protein, 20 mM phosphate buffer (pH 7.0), 5 mM lactose) and the reservoir solution (2.0 M ammonium sulfate). Data collection was carried out using synchrotron radiation at SPring-8 (Harima, Japan) and the Photon Factory (Tsukuba, Japan), and the data used for structure determination were collected

**Table II.** Data collection and refinement statistics

Temperature (K)	100
Resolution (Å)	1.86
Number of measured refs.	193,703
Number of unique refs.	26,434
$R_{\text{merge}}^a$	0.051 (0.173) <sup>b</sup>
$I/\sigma(I)$	13.7
Space group	$P2_12_12_1$
Cell dimensions	
$a$ (Å) =	36.93
$b$ (Å) =	87.43
$c$ (Å) =	95.70
Structure Refinement	
Resolution range (Å)	34.02–1.86
Number of refs.	26,434
Completeness (%)	98.6 (96.8) <sup>b</sup>
$R_{\text{crystal}}$	0.218 (0.219) <sup>b</sup>
$R_{\text{free}}$	0.244 (0.261) <sup>b</sup>
rmsd bond lengths (Å)	0.005
rmsd bond angles (°)	1.3

<sup>a</sup> $R_{\text{merge}} = \sum \sum |I_i - \langle I \rangle| / \sum \langle I \rangle$ .

<sup>b</sup>The values for the highest resolution shell (1.93–1.86 Å) are given in parentheses.

with an ADSC Quantum 4R CCD detector system on the BL-6A in the Photon Factory. The collected data were processed using the program HKL2000 (Otwinowski and Minor 1997). The collected data statistics are listed in Table II. The structure of the CSGal-1/lactose complex was determined by a molecular replacement method with the program CNS (Brunger et al. 1998), using the structure of human Gal-1 (PDB code 1GZW) as a search model. Further model building was performed with the program X-fit (McRee 1999), and the structure was refined using the program CNS (Brunger et al. 1998). Water molecules were gradually introduced if the peaks above  $4.0 \sigma$  in the ( $F_o - F_c$ ) electron density map were in the range of a hydrogen bond. After several cycles of positional and temperature factor refinements, a model was refined to a  $R_{\text{crystal}}$  of 0.218 with a good chemical geometry, as listed in Table II. The atomic coordinates and structure factors for the CSGal-1/lactose complex have been deposited in the Protein Data Bank under accession code 2ZKN.

#### **Supplementary Data**

Supplementary data for this article is available online at <http://glycob.oxfordjournals.org/>.

#### **Funding**

This study was supported in part by the National Project on Protein Structural and Functional Analyses from the Ministry of Education, Culture, Sports, Science and Technology of Japan.

#### **Acknowledgement**

The data collection was performed with the approval of the Photon Factory Advisory Committee, and SPring-8.



**Conflict of interest statement.**

None declared.

**Abbreviations**

CSGal-1, galectin-1-Cys3,17,43,61,89,131Ser; DTT, dithiothreitol; FAC, frontal affinity chromatography; Gal-1, galectin-1; LNFP-I, lacto-*N*-fucopentaose I; PA-oligosaccharides, pyridylamino-oligosaccharides; PMSF, phenylmethylsulfonyl fluoride; SDS-PAGE, sodium dodecyl sulfate-polyacrylamide gel electrophoresis.

**References**

- Barondes SH, Castronovo V, Cooper DN, Cummings RD, Drickamer K, Feizi T, Gitt MA, Hirabayashi J, Hughes C, Kasai K, et al. 1994. Galectins: A family of animal beta-galactoside-binding lectins. *Cell*. 76:597–598.
- Baum LG, Blackall DP, Arias-Magallano S, Nanigian D, Uh SY, Browne JM, Hoffmann D, Emmanouilides CE, Territo MC, Baldwin GC. 2003. Amelioration of graft versus host disease by galectin-1. *Clin Immunol*. 109:295–307.
- Brunger AT, Adams PD, Clore GM, DeLano WL, Gros P, Grosse-Kunstleve RW, Jiang JS, Kuszewski J, Nilges M, Pannu NS, et al. 1998. Crystallography & NMR system: A new software suite for macromolecular structure determination. *Acta Crystallogr D Biol Crystallogr*. 54:905–921.
- Camby I, Le Mercier M, Lefranc F, Kiss R. 2006. Galectin-1: A small protein with major functions. *Glycobiology*. 16:137R–157R.
- Elola MT, Chiesa ME, Alberti AF, Mordoh J, Fink NE. 2005. Galectin-1 receptors in different cell types. *J Biomed Sci*. 12:13–29.
- Hernandez JD, Nguyen JT, He J, Wang W, Ardman B, Green JM, Fukuda M, Baum LG. 2006. Galectin-1 binds different CD43 glycoforms to cluster CD43 and regulate T cell death. *J Immunol*. 177:5328–5336.
- Hirabayashi J, Hashidate T, Arata Y, Nishi N, Nakamura T, Hirashima M, Urashima T, Oka T, Futai M, Muller WE, et al. 2002. Oligosaccharide specificity of galectins: A search by frontal affinity chromatography. *Biochim Biophys Acta*. 1572:232–254.
- Hirabayashi J, Kasai K. 1991. Effect of amino acid substitution by sited-directed mutagenesis on the carbohydrate recognition and stability of human 14-kDa beta-galactoside-binding lectin. *J Biol Chem*. 266:23648–23653.
- Horie H, Inagaki Y, Sohma Y, Nozawa R, Okawa K, Hasegawa M, Muramatsu N, Kawano H, Horie M, Koyama H, et al. 1999. Galectin-1 regulates initial axonal growth in peripheral nerves after axotomy. *J Neurosci*. 19:9964–9974.
- Horie H, Kadoya T, Hikawa N, Sango K, Inoue H, Takeshita K, Asawa R, Hiroi T, Sato M, Yoshioka T, et al. 2004. Oxidized galectin-1 stimulates macrophages to promote axonal regeneration in peripheral nerves after axotomy. *J Neurosci*. 24:1873–1880.
- Inagaki Y, Sohma Y, Horie H, Nozawa R, Kadoya T. 2000. Oxidized galectin-1 promotes axonal regeneration in peripheral nerves but does not possess lectin properties. *Eur J Biochem*. 267:2955–2964.
- Kraulis PJ. 1991. MOLSCRIPT: A program to produce both detailed and schematic plots of protein structures. *J Appl Crystallogr*. 24:946–950.
- Laskowski RA, MacArthur MW, Moss DS, Thornton JM. 1992. PROCHECK v2: Programs to Check the Stereochemical Quality of Protein Structures. Oxford, England: Oxford Molecular Ltd.
- Lopez-Lucendo MF, Solis D, Andre S, Hirabayashi J, Kasai K, Kaltner H, Gabius HJ, Romero A. 2004. Growth-regulatory human galectin-1: Crystallographic characterization of the structural changes induced by single-site mutations and their impact on the thermodynamics of ligand binding. *J Mol Biol*. 343:957–970.
- Lu LH, Nakagawa R, Kashio Y, Ito A, Shoji H, Nishi N, Hirashima M, Yamauchi A, Nakamura T. 2007. Characterization of galectin-9-induced death of Jurkat T cells. *J Biochem*. 141:157–172.
- McRee DE. 1999. XtalView/Xfit – A versatile program for manipulating atomic coordinates and electron density. *J Struct Biol*. 125:156–165.
- Merritt EA, Bacon DJ. 1997. Raster3D: Photorealistic molecular graphics. *Methods Enzymol*. 277:505–524.
- Nakamura-Tsuruta S, Uchiyama N, Hirabayashi J. 2006. High-throughput analysis of lectin-oligosaccharide interactions by automated frontal affinity chromatography. *Methods Enzymol*. 415:311–325.
- Nguyen JT, Evans DP, Galvan M, Pace KE, Leitenberg D, Bui TN, Baum LG. 2001. CD45 modulates galectin-1-induced T cell death: Regulation by expression of core 2 *O*-glycans. *J Immunol*. 167:5697–5707.
- Nishi N, Inui M, Miyanaka H, Oya H, Wada F. 1995. Western blot analysis of epidermal growth factor using gelatin-coated polyvinylidene difluoride membranes. *Anal Biochem*. 227:401–402.
- Nowak TP, Haywood PL, Barondes SH. 1976. Developmentally regulated lectin in embryonic chick muscle and a myogenic cell line. *Biochem Biophys Res Commun*. 68:650–657.
- Otwinowski Z, Minor W. 1997. Processing of X-ray diffraction data collected in oscillation mode. *Methods Enzymol*. 277:307–326.
- Pace KE, Hahn HP, Pang M, Nguyen JT, Baum LG. 2000. CD7 delivers a pro-apoptotic signal during galectin-1-induced T cell death. *J Immunol*. 165:2331–2334.
- Perillo NL, Pace KE, Seilhamer JJ, Baum LG. 1995. Apoptosis of T cells mediated by galectin-1. *Nature*. 378:736–739.
- Rabinovich GA. 2005. Galectin-1 as a potential cancer target. *Br J Cancer*. 92:1188–1192.
- Rabinovich GA, Baum LG, Tinari N, Paganelli R, Natoli C, Liu FT, Iacobelli S. 2002. Galectins and their ligands: Amplifiers, silencers or tuners of the inflammatory response? *Trends Immunol*. 23:313–320.
- Rabinovich GA, Daly G, Dreja H, Tailor H, Riera CM, Hirabayashi J, Chernajovsky Y. 1999. Recombinant galectin-1 and its genetic delivery suppress collagen-induced arthritis via T cell apoptosis. *J Exp Med*. 190:385–398.
- Ramachandran GN, Sasisekharan V. 1968. Conformation of polypeptides and proteins. *Adv Protein Chem*. 23:283–438.
- Santucci L, Fiorucci S, Cammilleri F, Servillo G, Federici B, Morelli A. 2000. Galectin-1 exerts immunomodulatory and protective effects on concanavalin A-induced hepatitis in mice. *Hepatology*. 31:399–406.
- Santucci L, Fiorucci S, Rubinstein N, Mencarelli A, Palazzetti B, Federici B, Rabinovich GA, Morelli A. 2003. Galectin-1 suppresses experimental colitis in mice. *Gastroenterology*. 124:1381–1394.
- Scott K, Weinberg C. 2004. Galectin-1: A bifunctional regulator of cellular proliferation. *Glycoconj J*. 19:467–477.
- Stowell SR, Karmakar S, Stowell CJ, Dias-Baruffi M, McEver RP, Cummings RD. 2007. Human galectin-1, -2, and -4 induce surface exposure of phosphatidylserine in activated human neutrophils but not in activated T cells. *Blood*. 109:219–227.
- Tracey BM, Feizi T, Abbott WM, Carruthers RA, Green BN, Lawson AM. 1992. Subunit molecular mass assignment of 14,654 Da to the soluble beta-galactoside-binding lectin from bovine heart muscle and demonstration of intramolecular disulfide bonding associated with oxidative inactivation. *J Biol Chem*. 267:10342–10347.
- Walzel H, Blach M, Hirabayashi J, Kasai KI, Brock J. 2000. Involvement of CD2 and CD3 in galectin-1 induced signaling in human Jurkat T-cells. *Glycobiology*. 10:131–140.
- Walzel H, Fahmi AA, Eldesouky MA, Abou-Eladab EF, Waitz G, Brock J, Tiedge M. 2006. Effects of *N*-glycan processing inhibitors on signaling events and induction of apoptosis in galectin-1-stimulated Jurkat T lymphocytes. *Glycobiology*. 16:1262–1271.